

Avalanche Breakdown Design Parameters in GaN

To cite this article: Zhongda Li *et al* 2013 *Jpn. J. Appl. Phys.* **52** 08JN05

View the [article online](#) for updates and enhancements.

You may also like

- [Coplanar metal–semiconductor–metal light-emitting devices with an n++ InGaN layer and their application to display](#)
H Long, Y P Zeng, Y Mei *et al.*
- [Effect of p-NiO and n-ZnSe interlayers on the efficiency of p-GaN/n-ZnO light-emitting diode structures](#)
Vadim P Sirkeli, Oktay Yilmazoglu, Franko Küppers *et al.*
- [Red Electroluminescence from Light Emitting Diodes Based on Eu-Doped ZnO Embedded in p-GaN/Al₂O₃/n-ZnO Heterostructures](#)
Jun Tatebayashi, Kazuto Nishimura, Shuhei Ichikawa *et al.*

Avalanche Breakdown Design Parameters in GaN

Zhongda Li, Vipindas Pala[†], and T. Paul Chow

Center for Integrated Electronics, Rensselaer Polytechnic Institute, Troy, NY 12180, U.S.A.

Received October 13, 2012; revised November 29, 2012; accepted December 4, 2012; published online May 20, 2013

We have studied the avalanche breakdown design parameters of GaN n+/p and p+/n junctions in the voltage range of 1.2 to 12 kV using numerical simulations and analytical calculations. Important analytical models regarding the relationships between breakdown voltages, depletion width, maximum junction electric field and doping concentrations have been extracted which shows very high consistency with the results from numerical simulations. These analytical models can be used as guidelines in the designing of GaN high voltage power devices. The multiplication factors M_n and M_p have also been obtained and the analytical models have been extracted. The results showed that in GaN, n+/p junction is better than p+/n for the main voltage blocking junction due to a sharper avalanche current increase.

© 2013 The Japan Society of Applied Physics

1. Introduction

GaN power switching devices are competitive in the voltage range of 1.2 kV and above when compared with its silicon counterparts, due to its $10\times$ higher critical electric field, and the ability to operate at temperatures above 250°C .¹⁾ GaN MOSFETs has been demonstrated with positive threshold voltage and superior breakdown voltage compared with silicon.²⁻⁴⁾ In the cases of GaN high electron mobility transistors (HEMTs),^{5,6)} metal-insulator-semiconductor (MIS) HEMTs,^{7,8)} MOS-channel HEMTs (MOS-HEMTs),⁹⁻¹³⁾ and gate injection transistor (GIT),¹⁴⁾ the high mobility and concentration of the two-dimensional electron gas (2DEG) at the AlGaIn/GaN interface gives more advantage to GaN over silicon. GaN vertical power transistors have also been demonstrated.¹⁵⁻¹⁸⁾ However, there have been few studies on the design of the breakdown voltage for GaN power devices.

For silicon power devices, there have been many analytical studies on the designing of the breakdown voltage (BV). In semiconductor p-n junctions, avalanche breakdown happens when the impact ionization integral reaches unity:¹⁹⁾

$$I = \int_0^w \alpha_p \exp\left[\int_0^x (\alpha_n - \alpha_p) dx'\right] dx = 1. \quad (1)$$

The impact ionization coefficients α_n or α_p stand for the number of electron-hole pairs that are generated per unit distance by a single electron or hole respectively travelling in the direction of the electric field, and they are functions of the electric field:

$$\alpha_n = a_n \exp\left(-\frac{b_n}{E}\right), \quad \alpha_p = a_p \exp\left(-\frac{b_p}{E}\right). \quad (2)$$

In silicon, to solve Eq. (1) analytically, the average impact ionization coefficients of electrons and holes (α_{eff} in cm^{-1}) has been fitted as a power law with the power n of 7 using Fulop's approximation:¹⁹⁾

$$\alpha_{\text{eff}} \cong 1.8 \times 10^{-35} E^7. \quad (3)$$

For the case of a silicon 1D abrupt p-n junction, integrating Eq. (3) yields the relation between breakdown voltage (BV in V), depletion width (W in cm), critical electric field (E_c in V/cm) and the doping concentration (N):

$$\text{BV} \cong 5.34 \times 10^{13} N^{-3/4}, \quad (4)$$

$$W \cong 2.67 \times 10^{10} N^{-7/8}, \quad (5)$$

$$E_c \cong 4.01 \times 10^3 N^{1/8}. \quad (6)$$

Similarly, Fulop's approximation for 4H-SiC yields n of 6, and the equations have also been obtained as follows:²⁰⁾

$$\alpha_{\text{eff}} \cong 1.746 \times 10^{-35} E^6, \quad (7)$$

$$\text{BV} \cong 4.766 \times 10^{14} N^{-5/7}, \quad (8)$$

$$W \cong 7.151 \times 10^{10} N^{-6/7}, \quad (9)$$

$$E_c \cong 1.333 \times 10^4 N^{1/7}. \quad (10)$$

These equations can be used as design guide and facilitate the designing of silicon or SiC power devices. However, there has been no such study for GaN to the authors' knowledge. In this paper, we have derived the avalanche breakdown design equations for GaN and extracted the design parameters, and compared the analytical results with numerical simulations. Further, we have also examined and compared the sharpness of the avalanche breakdown current-voltage (I - V) characteristics of GaN p+/n and n+/p junctions using numerical simulations, and extracted the empirical parameters.

2. GaN Breakdown Voltage Design Parameters

The electron and hole impact ionization coefficients in GaN are the functions of the electric field as shown in Fig. 1, and the relation is same as in Eq. (2). The impact ionization model parameters are shown in Table I.²¹⁾ The effective impact ionization coefficient (α_{eff}) has been used as the average of α_n and α_p [defined in Eq. (11)].²²⁾ Then α_{eff} vs critical field (E_c) has been fitted to a power law $\alpha_{\text{eff}} \sim E_c^n$ using Fulop's approximation. Because the fitted power n depends largely on the range of E_c that is chosen for the fitting, we have used numerical simulations to determine the critical fields for breakdown voltage between 1.2 and 12 kV, and obtained the range of 2.4 to 3.6 MV/cm. Fulop's approximation within this range of E_c gives the power of 9.22 as can be seen Fig. 2, which was higher than the previously reported value of 8.²³⁾

$$\alpha_{\text{eff}} = \frac{a_n - a_p}{\ln(a_n/a_p)}, \quad (11)$$

$$\alpha_{\text{eff}} = 8.96 \times 10^{-57} E_c^{9.22}. \quad (12)$$

For 1D GaN abrupt p-n junction, the design equations can be derived from Eq. (12):

[†]Present address: Cree Inc., Durham, NC 27703, U.S.A.

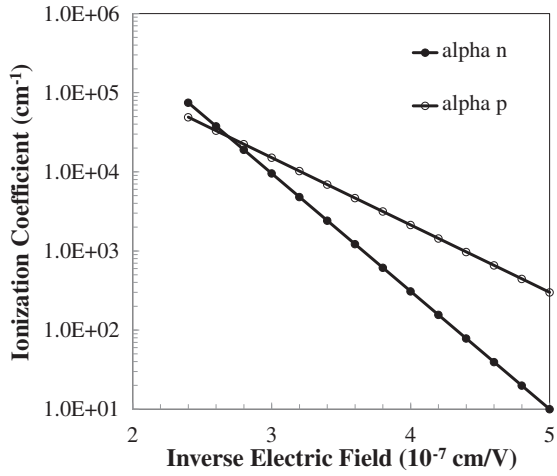


Fig. 1. Ionization coefficients vs inverse electric field for electrons and holes in GaN.

Table I. Impact ionization model parameters of GaN.

a_n (cm^{-1})	a_p (cm^{-1})	b_n (V/cm)	b_p (V/cm)
2.81×10^8	5.41×10^6	3.43×10^7	1.96×10^7

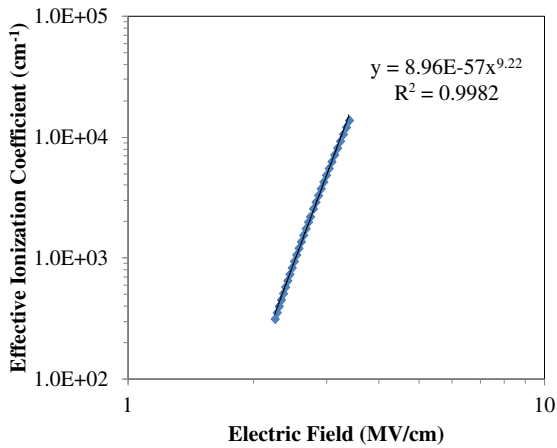


Fig. 2. (Color online) Effective ionization coefficient of GaN vs electric field approximated as a power law.

$$BV \cong 1.86 \times 10^{16} N^{-8.22/10.22} = 1.86 \times 10^{16} N^{-0.80}, \quad (13)$$

$$W \cong 4.42 \times 10^{11} N^{-9.22/10.22} = 4.42 \times 10^{11} N^{-0.90}, \quad (14)$$

$$E_c \cong 8.42 \times 10^4 N^{1/10.22} = 8.42 \times 10^4 N^{0.098}. \quad (15)$$

Numerical simulations using MEDICI have been performed to check the accuracy of the design equations. GaN impact ionization coefficients in Table I have been used in the numerical simulations. To facilitate convergence, photo generation method has been used in the simulations. Both GaN p+/n and n+/p junctions have been simulated and the breakdown voltages have been obtained. Figure 3 shows that for both p+/n and n+/p junctions, the simulated BV results match the analytical results with very

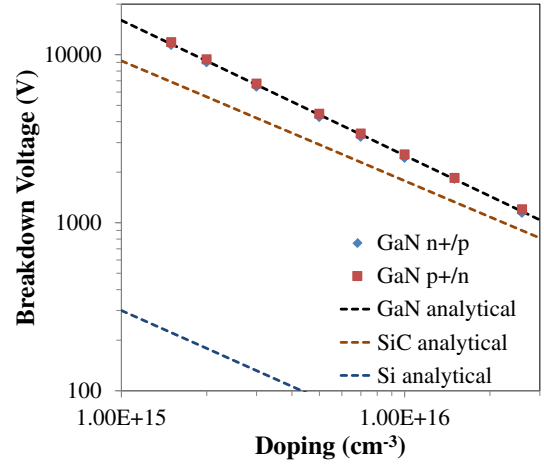


Fig. 3. (Color online) Breakdown voltage vs doping for GaN p+/n and n+/p junctions from simulations.

high accuracy in the voltage range of 1.2 to 12 kV. E_c calculated using Eq. (15) is also self-consistent with the range of E_c that is chosen for the Fulop's approximation in this voltage range.

3. GaN Avalanche Multiplication Factors

The avalanche multiplication factor, $M(x)$, is defined as the average total number of electron-hole pairs generated at a point of x within the depletion layer of a p-n junction.¹⁹⁾ M reaches infinity at breakdown voltage, and it determines the shape of the pre-breakdown I - V characteristics. For a p-n junction with the boundary between the neutral n region and the depletion region at $x = 0$, and the boundary between the neutral p region and the depletion region at $x = w$, at the location of $x = 0$, $M(0)$ is denoted as M_p because the current is dominated by diffusion current of holes (I_{p0}); and similarly at $x = w$, $M(w)$ is denoted as M_n . The multiplication factor of the generation current that exists in the whole space charge region, I_{sc} , is denoted as M_{sc} . Thus the total current multiplication can be represented as²²⁾

$$I = I_{p0}M_p + I_{n0}M_n + I_{sc}M_{sc}. \quad (16)$$

For n+/p junctions $M_{sc} \approx M_n$,¹⁹⁾ due to the fact that in a n+/p diode, the space charge region is mostly in the p type region, thus all the electrons generated in the space charge region are swept towards the peak field, while the holes are swept towards the low field direction. Similarly, for p+/n junctions, $M_{sc} \approx M_p$. For GaN, because of its extremely low intrinsic concentration due to the wide band-gap, the diffusion currents are negligible. Therefore for GaN n+/p junctions:

$$I \cong I_{sc}M_n. \quad (17)$$

And for GaN p+/n junctions:

$$I \cong I_{sc}M_p. \quad (18)$$

For silicon, it has been known that M_n and M_p can be approximated by

$$M = \frac{1}{1 - (V_j/BV)^m}, \quad (19)$$

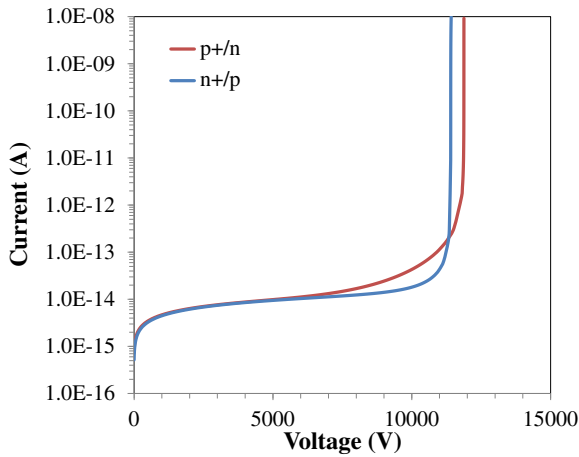


Fig. 4. (Color online) Breakdown I - V characteristics of GaN p+/n and n+/p junctions with doping of $2.6 \times 10^{16} \text{ cm}^{-3}$ from simulations.

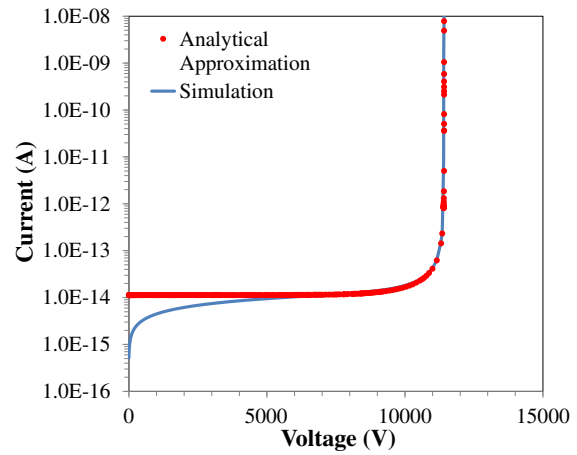


Fig. 5. (Color online) Fitting of the breakdown I - V characteristics of GaN n+/p junction from simulation with analytical approximation.

where for M_n , $m = 4$; for M_p , $m = 6$.¹⁹⁾ Higher m value results in sharper breakdown I - V characteristics, which means less power loss near the breakdown voltage. The m is also related to the BV of BJTs in terms of

$$\frac{BV_{ceo}}{BV_{cbo}} = \frac{1}{(1 + \beta)^{1/m}}, \quad (20)$$

where BV_{cbo} is the open emitter breakdown voltage, BV_{ceo} is the open base breakdown voltage, and β is the gain of the BJT. The factor m has been extracted for SiC BJTs to be around 8 to 10.²⁴⁾

Figure 4 shows the breakdown I - V characteristics for GaN n+/p and p+/n junctions with the doping of $2.6 \times 10^{16} \text{ cm}^{-3}$ from numerical simulations. The BV of GaN p+/n junction is slightly higher than the n+/p junction with the same doping. This happens because that for p+/n junctions, the impact ionization is dominated by the carrier multiplication initiated by the holes near the peak field, while for n+/p junctions is dominated by electrons. From Fig. 1, when electric field is high which is close to the peak field, α_p is lower than α_n and as a result, BV of GaN p+/n junction is higher than GaN n+/p junction. GaN n+/p junction shows a sharper breakdown I - V than the p+/n junction which indicates a larger factor m . Figure 5 shows the simulated breakdown I - V characteristics fitted to the analytical expression as in Eq. (19), showing high accuracy. The extracted m factor for GaN n+/p and p+/n junctions varies as a function of the breakdown voltage. Figure 6 shows that for GaN n+/p junctions, m increases from 5.7 to 8.5 for BV of 1.2 to 12 kV; while for GaN p+/n junctions, m decreases from 1.9 to 1.8. The factor m has also been obtained from calculating of the ionization integral numerically, and compared with that obtained from the numerical simulations. The two methods show similar values for the factor m with the same trend with increasing breakdown voltage. The slight difference may be attributed to that the ionization integral calculation method lacks the field modification by the carriers in transient and thus is less accurate compared with numerical simulations.

The higher m value of GaN n+/p junction suggests that GaN n+/p is the better choice to be used for the main

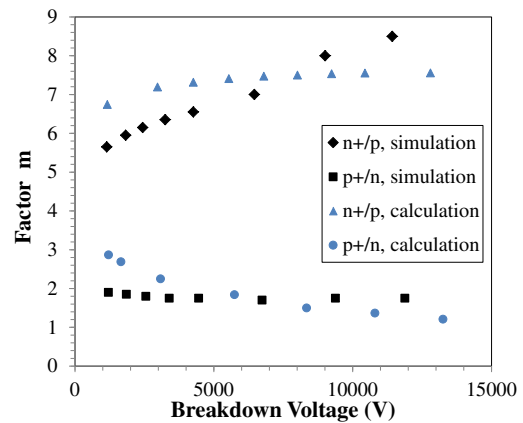


Fig. 6. (Color online) Factor m vs breakdown voltage for GaN p+/n and n+/p junctions from simulations and calculation of ionization integral.

voltage blocking junction. Further, the ratio of BV_{ceo}/BV_{cbo} of GaN pnp power BJTs is expected to be higher than that of the npn BJTs with the same gain (β).

4. Summary

In summary, we have studied the avalanche design parameters in GaN using numerical simulations and analytical calculations. The design equations for the relations between breakdown voltage, doping concentration, depletion width and the critical electric field have been obtained. The avalanche multiplication factor of GaN has also been extracted, and the result suggests that GaN n+/p junctions are the better candidate for voltage blocking junctions due to its sharper breakdown I - V .

Acknowledgement

This work was supported primarily by the Engineering Research Centers Program (ERC) of the National Science Foundation under NSF Cooperative Agreement No. EEC-0812056 and in part by New York State under NYSTAR contract C090145.

- 1) T. P. Chow and Z. Li: in *Springer Series in Materials Science*, ed. S. Pearton (Springer, New York, 2012) Vol. 156, Chap. 8.
- 2) K. Matocha, T. P. Chow, and R. J. Gutmann: *IEEE Electron Device Lett.* **52** (2005) 6.
- 3) W. Huang, T. Khan, and T. P. Chow: *IEEE Electron Device Lett.* **27** (2006) 796.
- 4) Y. Niiyama, Z. Li, T. P. Chow, J. Li, T. Nomura, and S. Kato: *Solid-State Electron.* **56** (2011) 73.
- 5) A. Nakajima, Y. Sumida, M. H. Dhyani, H. Kawai, and E. M. Sankara Narayanan: *IEEE Electron Device Lett.* **32** (2011) 542.
- 6) R. Chu, Z. Chen, S. P. DenBaars, and U. K. Mishra: *IEEE Electron Device Lett.* **29** (2008) 1184.
- 7) M. Kanamura, T. Ohki, T. Kikkawa, K. Imanishi, T. Imada, A. Yamada, and N. Hara: *IEEE Electron Device Lett.* **31** (2010) 189.
- 8) T. Oka and T. Nozawa: *IEEE Electron Device Lett.* **29** (2008) 668.
- 9) W. Huang, Z. Li, T. P. Chow, Y. Niiyama, T. Nomura, and S. Yoshida: *Proc. Int. Symp. Power Semicond. Device ICs, 2008*, p. 295.
- 10) K. Tang, Z. Li, T. P. Chow, Y. Niiyama, T. Nomura, and S. Yoshida: *Proc. Int. Symp. Power Semicond. Device ICs, 2009*, p. 279.
- 11) Z. Li, J. Waldron, R. Dayal, L. Parsa, M. Hella, and T. P. Chow: *Proc. Int. Symp. Power Semicond. Device ICs, 2012*, p. 45.
- 12) B. Lu, E. Matioli, and T. Palacios: *IEEE Electron Device Lett.* **33** (2012) 360.
- 13) M. Kuraguchi, Y. Takada, T. Suzuki, M. Hirose, K. Tsuda, W. Saito, Y. Saito, and I. Omura: *Phys. Status Solidi A* **204** (2007) 2010.
- 14) Y. Uemoto, M. Hikita, H. Ueno, H. Matsuo, H. Ishida, M. Yanagihara, T. Ueda, T. Tanaka, and D. Ueda: *IEEE Trans. Electron Devices* **54** (2007) 3393.
- 15) M. Kanechika, M. Sugimoto, N. Soejima, H. Ueda, O. Ishiguro, M. Kodama, E. Hayashi, K. Itoh, T. Uesugi, and T. Kachi: *Jpn. J. Appl. Phys.* **46** (2007) L503.
- 16) H. Otake, S. Egami, H. Ohta, Y. Nanishi, and H. Takasu: *Jpn. J. Appl. Phys.* **46** (2007) L599.
- 17) S. Chowdhury, M. H. Wong, B. L. Swenson, and U. K. Mishra: *IEEE Electron Device Lett.* **33** (2012) 41.
- 18) Y. Uemoto, D. Shibata, M. Yanagihara, H. Ishida, H. Matsuo, S. Nagai, N. Batta, M. Li, T. Ueda, T. Tanaka, and D. Ueda: *IEDM Tech. Dig., 2007*, p. 861.
- 19) S. K. Ghandhi: *Semiconductor Power Devices* (Wiley, New York, 1977) p. 38–46.
- 20) Y. Tang: Dr. Thesis, Faculty of Electrical Engineering, Rensselaer Polytechnic Institute, Troy, NY (2003).
- 21) I. H. Oğuzman, E. Bellotti, K. F. Brennan, J. Kolnik, R. Wang, and P. P. Ruden: *J. Appl. Phys.* **81** (1997) 7827.
- 22) J. Lutz, H. Schlangenotto, U. Scheuermann, and R. De Doncker: *Semiconductor Power Devices* (Springer, Heidelberg, 2011) p. 61–103.
- 23) K. Matocha: Dr. Thesis, Faculty of Electrical Engineering, Rensselaer Polytechnic Institute, Troy, NY (2003).
- 24) S. Balachandran, T. P. Chow, A. Agarwal, S. Scozzie, and K. A. Jones: *Mater. Sci. Forum* **483–485** (2005) 893.